

Thermal properties of polycrystalline $[\text{Mn}(\text{NH}_3)_6](\text{ClO}_4)_2$

Crystal structure and phase transitions

Joanna Hetmańczyk · Łukasz Hetmańczyk ·
Anna Migdał-Mikuli · Edward Mikuli

Received: 1 November 2013 / Accepted: 27 March 2014 / Published online: 27 April 2014
© The Author(s) 2014. This article is published with open access at Springerlink.com

Abstract The X-ray powder diffraction (XRPD) pattern of $[\text{Mn}(\text{NH}_3)_6](\text{ClO}_4)_2$ at room temperature can be indexed in the regular (cubic) system ($\text{Fm}\bar{3}\text{m}$ space group) with lattice cell parameter $a = 11.5729 \text{ \AA}$ and with four molecules per unit cell. The XRPD pattern at 100 K is evidently different, and it indicates lowering of the crystal structure. One phase transition at $T_{\text{C1}}^{\text{h}} = 143.5 \text{ K}$ (on heating) and at $T_{\text{C1}}^{\text{c}} = 137.6 \text{ K}$ (on cooling) was detected by DSC for $[\text{Mn}(\text{NH}_3)_6](\text{ClO}_4)_2$ in the range of 120–300 K. The following thermodynamic parameters for phase I \leftrightarrow phase II transition were obtained: $\Delta H = 3.1 \pm 0.2 \text{ kJ mol}^{-1}$ and $\Delta S = 21.6 \pm 0.3 \text{ J mol}^{-1} \text{ K}^{-1}$. The large value of entropy changes (ΔS) indicates considerable configurational disorder in the high temperature phase. The presence of 5.9 K hysteresis of the phase transition temperature at T_{C} and sharpness of the heat flow anomaly attest that the detected phase transition is of the first-order type. Appearing of the two new bands (splitting of $\delta_{\text{s}}(\text{HNH})F_{1\text{u}}$ mode) in FT-MIR spectra at the vicinity of 1200 cm^{-1} suggests that the phase transition undergoes a change of the crystal structure.

Keywords Hexaamminemanganese(II) perchlorate · Thermal decomposition (TG/DTG/QMS) · Phase transition · DSC · X-ray powder diffraction (XRPD) · FT-IR

Introduction

All up to now investigated ionic coordination compounds of the type $[\text{M}(\text{NH}_3)_6](\text{ClO}_4)_2$, where $\text{M} = \text{Mg}^{2+}$, Ca^{2+} , Fe^{2+} , Co^{2+} , Ni^{2+} and Cd^{2+} possess similar and very specific polymorphism [1–6]. All of them owned cubic symmetry of the crystal lattice ($\text{Fm}\bar{3}\text{m}$) of the high (room) temperature phase [7]. Phase transition at T_{C1} , connected with the large entropy change, was connected with the change of the crystal structure (mainly to the monoclinic phase; space group $\text{P}2_1/\text{c}$) and also with a drastic change of the speed of reorientational motions of ClO_4^- anions [1, 8, 9]. It was thought interesting to see whether a compound of the same type but with different cations $\text{M} = \text{Mn}^{2+}$ will possess a structure at room temperature and a phase polymorphism similar to that of those compounds just mentioned. So far, no data have been available about the crystal structure of $[\text{Mn}(\text{NH}_3)_6](\text{ClO}_4)_2$. Our results of X-ray investigations (XRPD) of the crystal structure of investigated compound in the room temperature (RT) phase are presented in [Results and discussion](#) of this paper.

The general aim of the present study is to investigate the polymorphism of $[\text{Mn}(\text{NH}_3)_6](\text{ClO}_4)_2$ in the temperature range of 120–300 K and find the connections of recorded phase transitions with eventual changes of the crystal structure. For this purpose, we employed besides XRPD also Fourier transforms middle-infrared spectroscopy (FT-MIR). In addition, we would like to obtain a better understanding of mechanisms of thermal decomposition of the title compound, particularly of its deamination processes. The results of thermal analysis of $[\text{Mn}(\text{NH}_3)_6](\text{ClO}_4)_2$ have been described in the literature [10]. It undergoes in two steps at ca. 373 K $[\text{Mn}(\text{NH}_3)_6](\text{ClO}_4)_2$, four molecules of ammonia per one

J. Hetmańczyk (✉) · Ł. Hetmańczyk · A. Migdał-Mikuli · E. Mikuli
Department of Chemical Physics, Faculty of Chemistry,
Jagiellonian University, ul. Ingardena 3, 30-060 Cracow, Poland
e-mail: serwonsk@chemia.uj.edu.pl

J. Hetmańczyk · Ł. Hetmańczyk
Frank Laboratory of Neutron Physics, Joint Institute for Nuclear
Research, 141980 Dubna, Russian Federation

formula unit were freeing, above 493 K investigated compound exploded.

Experimental

The examined compound $[\text{Mn}(\text{NH}_3)_6](\text{ClO}_4)_2$ was obtained from manganese(II) perchlorate hydrate $(\text{Mn}(\text{ClO}_4)_2 \cdot x\text{H}_2\text{O})$ purchased from Sigma-Aldrich company. The $\text{Mn}(\text{ClO}_4)_2 \cdot x\text{H}_2\text{O}$ complex was placed in a quartz vessel and put in a glass tube, through which dry gaseous ammonia was blown, and the tube was placed in an oven, according to the method proposed by Smith and Koch [11]. First, the tube was heated for several days up to about 400 K until the water molecule from $[\text{Mn}(\text{H}_2\text{O})_x](\text{ClO}_4)_2$ was lost, and hexamine complex was composed. Then, after cooling the tube to room temperature, the obtained compound was put into a desiccator for several hours in order to get rid of ammonia excess. Before the measurements were taken, the composition of the compound under study was determined based on its ammonia content by titration using HCl. The average content of NH_3 was found to be equal to the theoretical values within the error limit of ca. 2 %.

X-ray powder diffraction (XRPD) patterns were measured in a capillary spinning add-on using a PANalytical X'Pert PRO MPD diffractometer with X'Celerator detector operated at 40 kV, 30 mA $\text{CuK}\alpha$ radiation ($\lambda = 1.54178 \text{ \AA}$) with a step size of 0.02° . Variable temperature X-ray powder diffraction (VTXRD) measurements were performed in nitrogen atmosphere with the same diffractometer equipped with Oxford Cryostream system. Each powder pattern was recorded in the range of 3° – 80° (2θ).

Thermal gravimetry analysis (TG, DTG) with simultaneous differential thermal analyses (SDTA) measurements was performed using a Mettler-Toledo 851^e apparatus. Sample of mass 4.9826 mg was placed in a 150 μl open corundum crucible. The measurements were made in a flow of Argon (60 mL min^{-1}), within temperature range of 300–478 K. The TG measurements were performed at a constant heating rate of 10 K min^{-1} . The simultaneous evolved gas analysis (SEGA) was performed during the experiments by a joined on-line quadruple mass spectrometer (QMS) using a ThermoStar-Balzars apparatus. The temperature was measured by a Pt–Pt/Rh thermocouple with an accuracy of $\pm 0.5 \text{ K}$.

Differential scanning calorimetry (DSC) measurements in the temperature range of 120–723 K were performed using a Mettler-Toledo 822^e calorimeter. The sample of mass equals to 3.01 mg was placed in 40 μL aluminium container and closed by compression. The heating rate equals to 10 K min^{-1} . The DSC measurements below room temperature were performed using two different calorimeters. The first run (sample A, mass = 8.04 mg)

was made on a Perkin-Elmer DIAMOND 8000 DSC apparatus, whereas the second run (sample B, mass = 2.83 mg) was made on a Mettler-Toledo 822^e calorimeter, both runs were performed in range of 123–300 K. The DSC measurements were made both during heating and cooling of the sample at constant rates of 10 and 20 K min^{-1} for sample A and 5 K min^{-1} for sample B. Other experimental details were the same as those published in our previous paper [12].

Fourier transforms far and middle infrared (FT-FIR and FT-MIR) absorption measurements were performed using a Bruker Vertex 70v vacuum Fourier Transform spectrometer. The transmission spectra were collected with a resolution of 2 cm^{-1} and with 32 scans per each spectrum. The FT-FIR spectra (500 – 50 cm^{-1}) were collected for sample suspended in Apiezon N grease and placed on polyethylene (PE) disc. The FT-MIR spectra were collected for sample suspended in Nujol placed between KBr pellets. Temperature measurements were carried out using Advanced Research System cryostat DE-202A and water cooled helium compressor ARS-2HW working in a closed cycle manner. The sample was loaded at room temperature, and measurements were performed on cooling down to ca. 9 K. The desired temperature was measured with accuracy of $\pm 0.1 \text{ K}$ and stabilized for ca. 3 min before the measurements were taken. The LakeShore 331S temperature controller equipped with silicon diode sensor was used to control the temperature. The cooling rate between desired temperatures was ca. 3 K min^{-1} . The PE and KRS5 windows were used in a cryostat in the case of FT-FIR and FT-MIR measurements, respectively.

Results and discussion

Crystal structure of $[\text{Mn}(\text{NH}_3)_6](\text{ClO}_4)_2$ at 298 and 100 K

In order to confirm the identity of the title compound, the X-ray powder diffraction measurements (XRPD) at 298 and 100 K were performed. Figure 1a shows the diffraction pattern collected for $[\text{Mn}(\text{NH}_3)_6](\text{ClO}_4)_2$ at room temperature. The strong reflexes were indexed in a cubic system using CRYSFIRE package and TREOR indexing program [13, 14]. Analysis of the systematic absences led us to the conclusion that space group No. 225, $\text{Fm}\bar{3}\text{m}$, can be assigned. However, in the diffraction pattern, several very weak reflexes can be also noticed which cannot be explained by the suggested crystal system. The additional reflexes can be easily explained by assumption that during synthesis small amount of NH_4ClO_4 is also formed. This is not surprising because it is commonly known that Mn^{2+} ion is stable in slightly acidic environment. The titled compound is rather

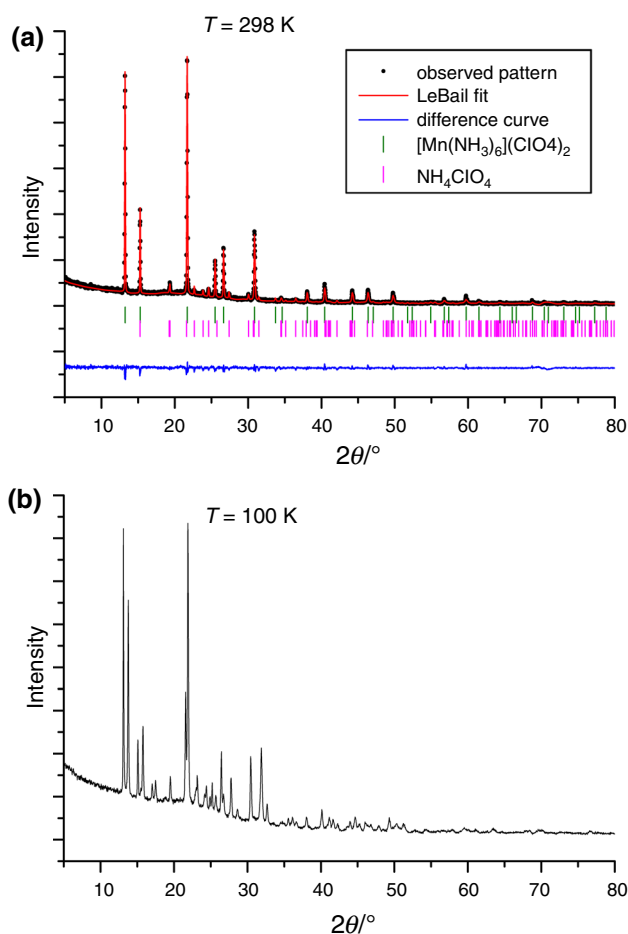


Fig. 1 X-ray powder diffraction pattern of $[\text{Mn}(\text{NH}_3)_6](\text{ClO}_4)_2$ registered at 298 K (a) and 100 K (b). (Color figure online)

unstable, and transformation to MnO_2 (dark grey colour of the sample) is observed within few days even for the sample which was kept hermetically closed. The manganese in its four oxidation states is stable in a neutral environment which is undoubtedly formed during process of ammonia blowing. We have performed whole pattern fitting including both components of the mixture using LeBail method [15] and FULLPROF [16] software in order to obtain lattice constants parameters. The lattice parameter $a = 11.5729 \text{ \AA}$ was obtained for chlorate(VII) hexaamminemanganese(II). The compound has a fluorite type structure, typical for K_2PtCl_6 with four molecules in the unit cell. The structure parameters are very similar to those proposed by Wyckoff [7] for other ionic hexaamminemetal(II) complexes. Figure 1a shows results of LeBail fitting performed for $[\text{Mn}(\text{NH}_3)_6](\text{ClO}_4)_2$ at RT, and Fig. 2 presents a view of the unit cell. The crystal structure consists of octahedral $[\text{Mn}(\text{NH}_3)_6]^{2+}$ cations and tetrahedral ClO_4^- anions. $[\text{Mn}(\text{NH}_3)_6](\text{ClO}_4)_2$ is isostructural with other similar complexes of the type $[\text{M}(\text{NH}_3)_6](\text{ClO}_4)_2$, where $\text{M} = \text{Mg}^{2+}, \text{Ca}^{2+}, \text{Fe}^{2+}, \text{Co}^{2+}, \text{Ni}^{2+}$ and Cd^{2+} .

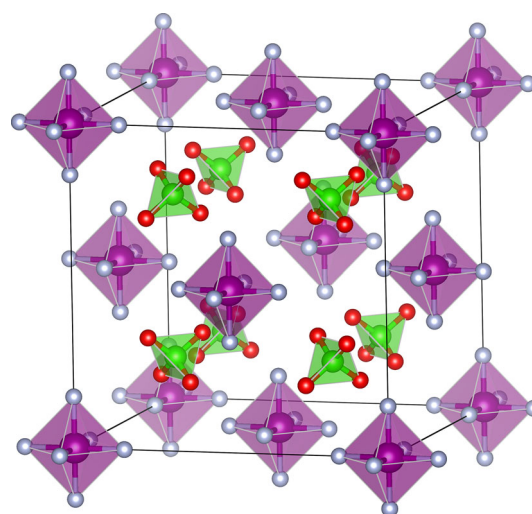


Fig. 2 View of the unit cell of $[\text{Mn}(\text{NH}_3)_6](\text{ClO}_4)_2$ at room temperature. (Color figure online)

Figure 1 shows a comparison of XRPD patterns registered for high and low temperature phases of the discussed compound. There are well-visible significant differences in the diffraction patterns registered at 298 K (high temperature phase I) and at 100 K (low temperature phase II). It indicates that crystal structure change occurs during the phase transition, which was registered by DSC at ca. 144 K (Phase transition investigations by DSC). Similar behaviour was also observed in the case of other members of hexaamminemetal(II) perchlorates, namely for $[\text{Ni}(\text{NH}_3)_6](\text{ClO}_4)_2$, $[\text{Mg}(\text{NH}_3)_6](\text{ClO}_4)_2$ and $[\text{Ca}(\text{NH}_3)_6](\text{ClO}_4)_2$ [1, 2, 4]. Unfortunately, bad quality of the $[\text{Mn}(\text{NH}_3)_6](\text{ClO}_4)_2$ diffraction pattern at 100 K precludes determination of crystal structure of the low temperature phase. Attempts to index this pattern were unsuccessful.

Characteristic dependence between the values of phase transition temperature T_{C1}^{h} and lattice parameter a for the compounds of the type $[\text{M}(\text{NH}_3)_6]\text{X}_2$ was first noticed by Stankowski [17]. The points on T_{C1}^{h} vs. a diagram for the complexes with different anions $\text{X}^- (\text{Cl}^-, \text{Br}^-, \text{J}^-, \text{ClO}_4^-, \text{BF}_4^-, \text{NO}_3^-, \text{PF}_6^-)$ fit in separate, characteristic for the type of the anion, areas in this diagram. Moreover, the anions with the structure of the highest symmetry have lower T_{C1}^{h} values than those of a lower symmetry (for example $T_{\text{C1}}^{\text{h}}(\text{NO}_3^-) > T_{\text{C1}}^{\text{h}}(\text{ClO}_4^-) > T_{\text{C1}}^{\text{h}}(\text{Cl}^-)$). Figure 3 presents T_{C1}^{h} vs. a^3 dependence for $[\text{M}(\text{NH}_3)_6](\text{ClO}_4)_2$, where $\text{M} = \text{Mg}^{2+}, \text{Ca}^{2+}, \text{Mn}^{2+}, \text{Fe}^{2+}, \text{Co}^{2+}, \text{Ni}^{2+}$ and Cd^{2+} . For a comparison, Fig. 3 includes also such dependences for $[\text{M}(\text{NH}_3)_6](\text{BF}_4)_2$ and $[\text{M}(\text{NH}_3)_6](\text{NO}_3)_2$ complexes. From our point of view, the volume of unit cell ($V = a^3$) is better parameter for such presentation than only a .

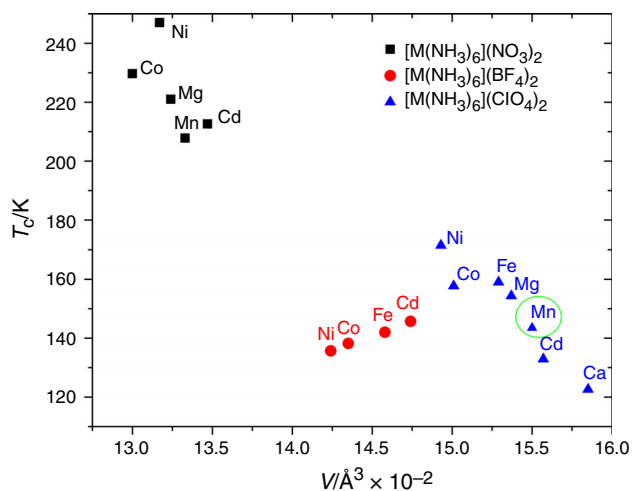


Fig. 3 T_{C1}^h versus volume of the unit cell ($V = a^3$) dependence for $[\text{M}(\text{NH}_3)_6](\text{ClO}_4)_2$ complexes, where $\text{M} = \text{Mg}^{2+}$, Ca^{2+} , Mn^{2+} , Fe^{2+} , Co^{2+} , Ni^{2+} and Cd^{2+} . For a comparison, such dependences for $[\text{M}(\text{NH}_3)_6](\text{BF}_4)_2$ and $[\text{M}(\text{NH}_3)_6](\text{NO}_3)_2$ complexes were added. (Color figure online)

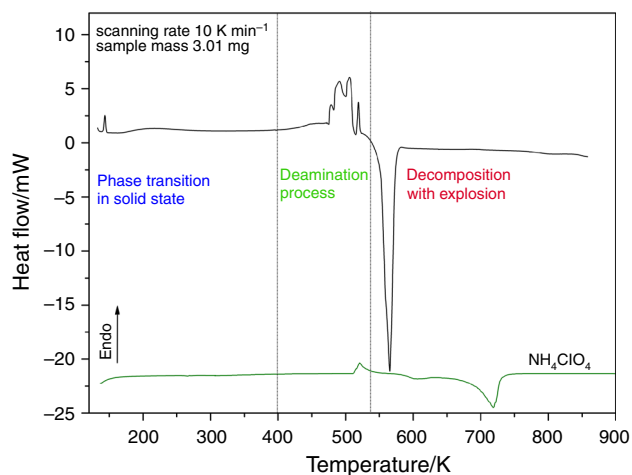


Fig. 4 DSC curve for $[\text{Mn}(\text{NH}_3)_6](\text{ClO}_4)_2$ registered at heating rate of 10 K min^{-1} in the temperature range of 120–900 K. Lower curve (green line) corresponds to pure NH_4ClO_4 . (Color figure online)

Thermal behaviour of the title compound (recognition by DSC, TG, DTG, QMS)

Figure 4 shows the DSC results obtained in the temperature range of 123–723 K with the scanning rate of 10 K min^{-1} for $[\text{Mn}(\text{NH}_3)_6](\text{ClO}_4)_2$ sample closed in aluminium vessel. This measurement was performed before TG analysis in order to check the stability of the compound and to qualitative comparison of these results with thermal analysis.

Three endothermic peaks clearly visible in DSC curve for $[\text{Mn}(\text{NH}_3)_6](\text{ClO}_4)_2$ in the temperature range of 400–515 K (Fig. 4) are associated with the liberation of almost

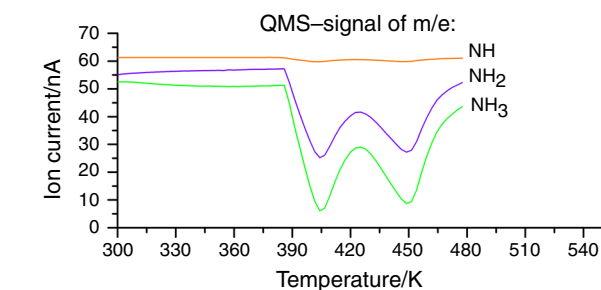
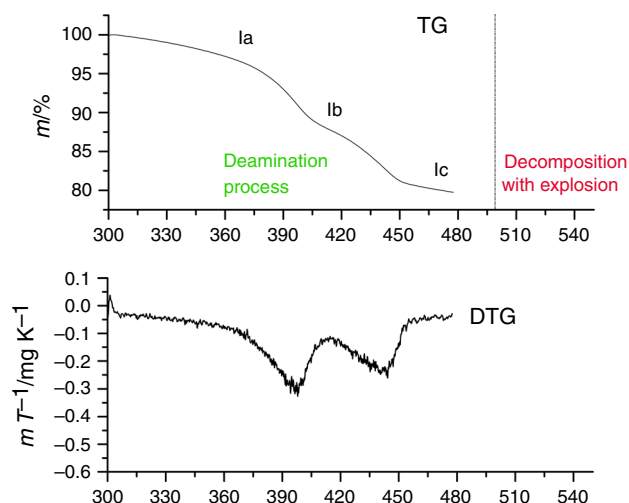
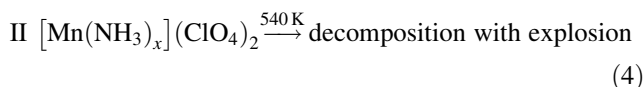
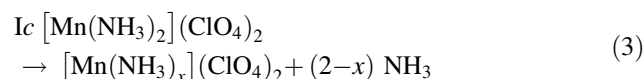
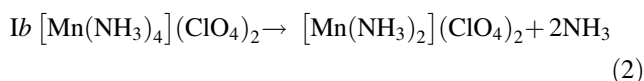
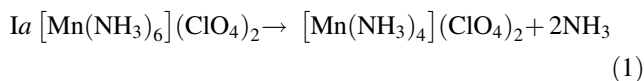


Fig. 5 TG, DTG and QMS curves for $[\text{Mn}(\text{NH}_3)_6](\text{ClO}_4)_2$ registered at heating rate of 10 K min^{-1} in the temperature range of 300–478 K. (Color figure online)

all NH_3 ligands. The process of deamination undergoes according to the following reactions:



Endothermic peak registered in DSC curve at 519 K is connected with the phase transition in solid state of NH_4ClO_4 , which in small amount is also formed during the synthesis of $[\text{Mn}(\text{NH}_3)_6](\text{ClO}_4)_2$. Above 538 K, we observed the decomposition with explosion of manganese(II) perchlorate.

Figure 5 presents TG, DTG and QMS curves recorded for $[\text{Mn}(\text{NH}_3)_6](\text{ClO}_4)_2$ at a constant heating rate of 10 K min^{-1} in the temperature range of 300–478 K (above this temperature sample explodes). During the TG

Table 1 Parameters of $[\text{Mn}(\text{NH}_3)_6](\text{ClO}_4)_2$ thermal analysis

Sample mass/mg	Stage number	Temperature range/K	Mass loss at the stage/%	Mass after decomposition/%	Calculated values/%	Products of the decomposition
4.9826	Ia	300–398	9.4		9.6	2 NH_3
	Ib	398–448	9.8		9.6	2 NH_3
	Ic	448–478	1.1			NH_3
	II	Above 540				Explosion

experiment, the QMS spectrum of masses was followed from $m/e = 1$ –100, however, for reasons of graphic readability, only the masses of $m/e = 15$, 16 and 17—representing NH , NH_2 and NH_3 are shown. The TG, DTG and QMS curves indicate that the deamination undergoes in the *three* steps (Ia, Ib and Ic). Statistically, at step Ia, 2 molecules of ammonia per one formula unit are freeing, the next 2 molecules of ammonia are freeing at step Ib and the rest in step Ic. The temperatures, percentage mass of losses and the products of the decomposition of $[\text{Mn}(\text{NH}_3)_6](\text{ClO}_4)_2$ at particular stages are presented in Table 1. The temperature ranges of sample transformation were taken from the DSC measurements. They are shifted with respect to TG measurements towards a little bit higher temperatures. The reason is slightly different conditions during measurements. The DSC was performed for sample closed in alumina vessel with micro-hole, whereas the TG investigations were performed in open crucible.

The results obtained in this paper differ slightly from those presented so far in the literature. The process of deamination is also different. From our study, it is clearly visible that $[\text{Mn}(\text{NH}_3)_6](\text{ClO}_4)_2$ firstly loses two molecules of ammonia, and next two molecules are freeing (step Ia and Ib). Further heating causes that not completely deaminated manganese(II) perchlorate decomposes with explosion at ca. 540 K. The temperature of explodes discovered by us is ca. 50 K higher than given in [10]. The explosion of the compounds containing perchlorate anion during the thermal decomposition is a common feature of these complexes: $[\text{Ca}(\text{NH}_3)_6](\text{ClO}_4)_2$ and $[\text{Sr}(\text{OS}(\text{CH}_3)_2)_6](\text{ClO}_4)_2$ [18, 19].

Comparing the thermal decomposition processes of $[\text{Mn}(\text{NH}_3)_6](\text{ClO}_4)_2$ and $[\text{Ca}(\text{NH}_3)_6](\text{ClO}_4)_2$ [18], registered at a constant heating rate in a flow of Argon, we noticed that they proceed in different ways. The main difference is in the temperature range in which all molecules of ammonia are freeing. It can be seen that in case of $[\text{Mn}(\text{NH}_3)_6](\text{ClO}_4)_2$, the particular NH_3 ligands are liberated in a much lower temperature (300–515 K) than the NH_3 in $[\text{Ca}(\text{NH}_3)_6](\text{ClO}_4)_2$ (341–601 K). The temperature of explosion discovered by us for $[\text{Mn}(\text{NH}_3)_6](\text{ClO}_4)_2$ is ca. 150 K lower than observed for $[\text{Ca}(\text{H}_2\text{O})_4](\text{ClO}_4)_2$ (above 700 K). Thermal decomposition of the investigated compound is similar to $[\text{Mn}(\text{NH}_3)](\text{NO}_3)_2$ [20] and $[\text{Ni}(\text{NH}_3)](\text{NO}_3)_2$ [21]. In both cases, not completely

deaminated manganese(II) and nickel(II) compounds, respectively, decomposed. In case of $[\text{Mn}(\text{NH}_3)](\text{NO}_3)_2$, deamination takes place at even lower temperature (ca. 450 K).

Phase transition investigations by DSC

Figure 6 presents the temperature dependence of the heat flow obtained for the title compound on heating (upper curve) and on cooling (down curve) for sample B of $[\text{Mn}(\text{NH}_3)_6](\text{ClO}_4)_2$ at the rate of 5 K min^{-1} . One distinct anomaly on each of these two DSC curves at $T_{\text{Cpeak}}^{\text{h}} = 143.6$ and $T_{\text{Cpeak}}^{\text{c}} = 137.8$ K (where indexes h and c denote heating and cooling of the sample, respectively). The pure NH_4ClO_4 does not exhibit any phase transition in that region (see for comparison in Fig. 4). These phase transition temperatures were calculated by extrapolating the corresponding dependencies of $T_{\text{Cpeak}}^{\text{h}}$ and $T_{\text{Cpeak}}^{\text{c}}$ values versus the scanning rate dependences, registered at scanning rates of heating and cooling the sample: 5, 10 and 20 K min^{-1} , to the scanning rate value equal to 0 K min^{-1} . The mean value of the phase transition temperature is $T_{\text{C1}}^{\text{h}} = 143.5$ K (on heating) and at $T_{\text{C1}}^{\text{c}} = 137.6$ K (on cooling) with the estimated entropy change $\Delta S = 21.6 \pm 0.3 \text{ J mol}^{-1} \text{ K}^{-1}$. The large transition entropy change indicates considerable configurational disorder in the high temperature phase (so called ODIC crystals [22]). The presence of 5.9 K hysteresis of the phase transition temperature at T_{C1} and sharpness of the anomaly attest that the detected phase transition is of the first-order type. Thus, the title compound has two solid phases in the temperature range of 123–300 K: high temperature (phase I) and low temperature phases (phase II). The thermodynamic parameters of the detected phase transition obtained during heating are presented in Table 2. The values of entropy change accompanying these phase transitions suggest also their ‘order–disorder’ mechanism.

Vibrational motions and phase transition

Vibrational FT-IR spectra for $[\text{Mn}(\text{NH}_3)_6](\text{ClO}_4)_2$ were measured as a function of temperature. The list of the band

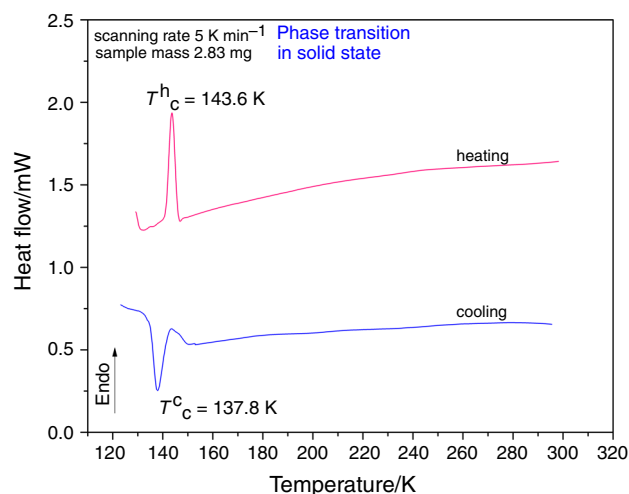


Fig. 6 DSC curve obtained for $[\text{Mn}(\text{NH}_3)_6](\text{ClO}_4)_2$ on heating (upper curve) and cooling (lower curve) with a scanning rate of 5 K min^{-1} . (Color figure online)

Table 2 Thermodynamic parameters of the phase transitions of $[\text{Mn}(\text{NH}_3)_6](\text{ClO}_4)_2$

Thermodynamics parameters	T_C/K	$\Delta H \pm \Delta\delta H/\text{kJ mol}^{-1}$	$\Delta S \pm \Delta\delta S/\text{J mol}^{-1} \text{K}^{-1}$
Heating	143.6 ± 0.1	3.1 ± 0.2	21.6 ± 0.3
Cooling	137.8 ± 0.1	3.0 ± 0.3	21.8 ± 0.3

positions, their relative intensities and tentative assignments are listed in Table 3. The assignments of these vibrations were proposed by comparing their frequencies with the literature data collected for titled compounds and similar ionic perchlorate aminometal(II) complexes [10, 23–27]. All characteristic bands frequencies of the internal vibrations were found. These assignments proved that the composition and structure of the investigated compound are correct. Detailed description and analysis of vibrational modes can be found in Mikuli et al. [20].

Figure 7 shows the FT-FIR spectra of $[\text{Mn}(\text{NH}_3)_6](\text{ClO}_4)_2$ within the wavenumber range of $500\text{--}50 \text{ cm}^{-1}$ registered during the cooling of the sample from 290 to 9 K. The spectrum at the lowest temperature contains seven bands. Three of them at 60, 68 and 76 cm^{-1} are associated with the ν_L lattice vibration modes. Next three bands at 184, 296 and 421 cm^{-1} are associated with the internal vibrations of $[\text{Mn}(\text{NH}_3)_6]^{2+}$ ion of the modes: $\delta_{\text{as}}(\text{NMnN})$, $\nu_{\text{as}}(\text{Mn-N})$ and $\nu_{\text{s}}(\text{Mn-N})$, respectively. Some interesting changes can be noticed for the band at 288 cm^{-1} (RT temperature) associated with stretching mode $\nu_{\text{as}}(\text{Mn-N})F_{1u}$. Apart from narrowing of this band,

Table 3 The list of band positions of the infrared spectra of $[\text{Mn}(\text{NH}_3)_6](\text{ClO}_4)_2$ at room temperature (*vw* very weak, *w* weak, *sh* shoulder, *m* medium, *st* strong, *vst* very strong, *br* broad)

Frequencies of vibrations/ cm^{-1}		Assignments
IR at 295 K	IR at 9 K	
3385 m	3388 st	$\nu_{\text{as}}(\text{NH})F_{1u}$
3293 m	3295 m	$\nu_{\text{s}}(\text{NH})F_{1u}$
	3265 m	$\nu_{\text{s}}(\text{NH})F_{1u}$
3189 sh	3200 sh	$\nu_{\text{s}}(\text{NH})F_{1u}$
	1616 vw	$\delta_{\text{as}}(\text{HNN})F_{1u}$
1609 m	1605 m	$\delta_{\text{as}}(\text{HNN})F_{1u}$
	1595 vw	$\delta_{\text{as}}(\text{HNN})F_{1u}$
1303 w	1300 w	$\delta_{\text{s}}(\text{HNN})A_{1g}$
1205 m	1197 m	$\delta_{\text{s}}(\text{HNN})F_{1u}$
	1172 vw	$\delta_{\text{s}}(\text{HNN})F_{1u}$
	1161 w	$\delta_{\text{s}}(\text{HNN})F_{1u}$
1092 vst	1086 vst	$\nu_{\text{as}}(\text{ClO})F_2$
937 vw	935 vw	$\nu_{\text{s}}(\text{ClO})A_1$
916 vw	915 vw	$2\delta(\text{OCIO})E + A_1$
894 vw	889 vw	$2\delta(\text{OCIO})E + A_1$
768 vw	767 vw	
626 m	627 m	$\delta_{\text{d}}(\text{OCIO})F_2$
591 m	594 m	$\rho_{\text{r}}(\text{NH}_3)F_{1u}$
	460 vw	$\delta_{\text{d}}(\text{OCIO})E$
417 br	421 br	$\nu_{\text{s}}(\text{Mn-N})A_{1g}$
283 m	296 m	$\nu_{\text{as}}(\text{Mn-N})F_{1u}$
179 st	184 st	$\delta_{\text{as}}(\text{NMnN})F_{1u}$
76 st	76 st	$\nu_L(\text{lattice})E_g$
70 v	68 st	$\nu_L(\text{lattice})E_g$
60 vw	60 vw	$\nu_L(\text{lattice})E_g$

the shifting towards higher wavenumbers is visible during the cooling of the sample, especially in the region of the phase transition. The last band at 460 cm^{-1} is connected with the ClO_4^- anion normal mode $\delta_{\text{d}}(\text{OCIO})E$.

The temperature-dependent FT-MIR spectra were also recorded during a cooling of the sample. Figure 8 shows exemplarily the spectra in the wavenumber ranges: $4000\text{--}3040$, $1840\text{--}1500$ and $1300\text{--}500 \text{ cm}^{-1}$, at selected temperatures of measurement. Some evident changes in the spectra at the temperature region of the phase transition can be noticed. Namely, apart from the narrowing, the splitting of some bands can be seen below the phase transition. As one can see in Fig. 8, new bands start to appear in the spectra on cooling just after the phase transition temperature (at ca. 130 K) in the wavenumber range ($1200\text{--}1150 \text{ cm}^{-1}$), connected with the $\delta_{\text{s}}(\text{HNN})F_{1u}$ mode. Thus, according to the infrared spectroscopy point of view, a change of the point symmetry takes place at the phase transition.

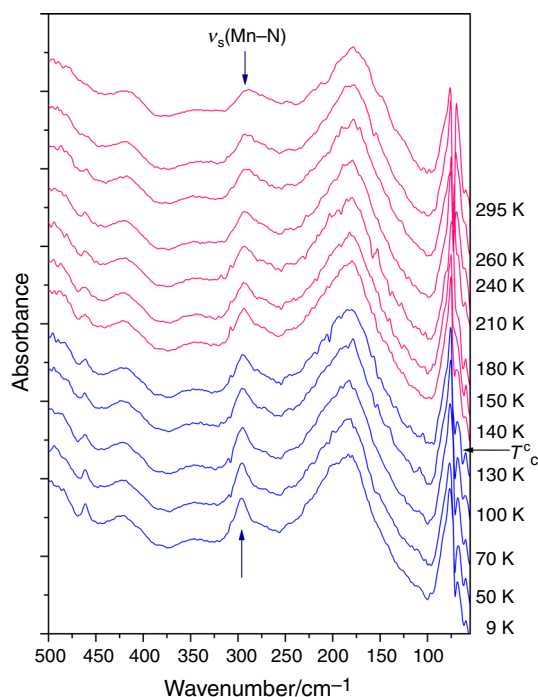


Fig. 7 Selected FT-FIR spectra in the wavenumber range of 500–50 cm^{-1} at different temperatures registered at cooling of the $[\text{Mn}(\text{NH}_3)_6](\text{ClO}_4)_2$. Phase transition temperature registered by DSC also at cooling is indicated by arrow. (Color figure online)

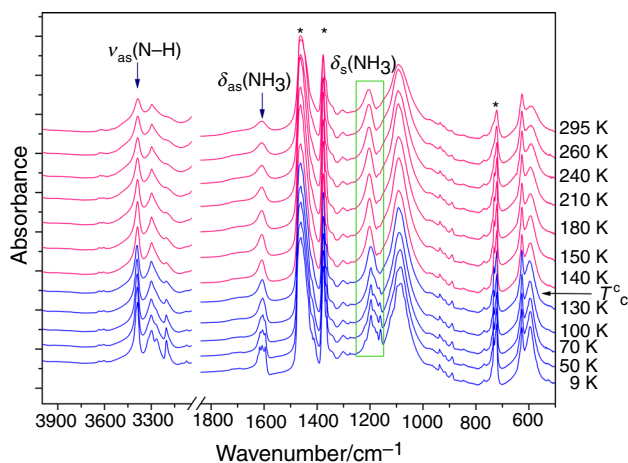


Fig. 8 Middle infrared spectra in the wavenumber ranges: 4000–3040, 1840–1500 and 1300–500 cm^{-1} at different selected temperatures (at cooling of the $[\text{Mn}(\text{NH}_3)_6](\text{ClO}_4)_2$ sample in Nujol). Phase transition temperature registered by DSC also at cooling is indicated by arrow. (Color figure online)

The narrowing of $\delta_{\text{as}}(\text{HNH})F_{1u}$ (1628 cm^{-1}) and $\nu_{\text{as}}(\text{NH})F_{1u}$ (3385 cm^{-1}), bands with temperature decreasing, indicates slowing of their fast reorientational motions in the vicinity of phase transition.

Conclusions

The results obtained in this work and their comparison with the literature data led us to the following conclusions:

X-ray powder diffraction (XRPD) measurement at room temperature indicated that $[\text{Mn}(\text{NH}_3)_6](\text{ClO}_4)_2$ has a structure of cubic symmetry (space group: $\text{Fm}\bar{3}\text{m}$, No. 225) with four molecules in the unit cell and lattice parameter $a = 11.5729 \text{ \AA}$. The crystal structure consists of octahedral $[\text{Mn}(\text{NH}_3)_6]^{2+}$ cations and tetrahedral ClO_4^- anions. $[\text{Mn}(\text{NH}_3)_6](\text{ClO}_4)_2$ is isostructural with the $[\text{M}(\text{NH}_3)_6](\text{ClO}_4)_2$ compounds that are studied earlier by us. XRPD pattern registered at 298 K (high temperature phase I) is different than that obtained at 100 K (low temperature phase II). Changes observed in diffraction patterns of $[\text{Mn}(\text{NH}_3)_6](\text{ClO}_4)_2$ suggest that the phase transition at $T_{\text{C}1}^{\text{c}}$ is associated with a change of the crystal structure.

Differential scanning calorimetry (DSC) measurements of $[\text{Mn}(\text{NH}_3)_6](\text{ClO}_4)_2$ performed in the temperature range of 123–295 K allowed to detect one solid–solid phase transition. The temperature of this phase transition amount to $T_{\text{C}1}^{\text{h}} = 143.5 \text{ K}$ (on heating) and at $T_{\text{C}1}^{\text{c}} = 137.6 \text{ K}$ (on cooling). Thermal hysteresis of the phase transition temperature ($\Delta T_{\text{C}} \approx 5.9 \text{ K}$) and entropy change value ($\Delta S = 21.6 \text{ J mol}^{-1} \text{ K}^{-1}$) connected with this phase transition indicate that it is of a first-order type, suggest that it is of ‘order–disorder’ mechanism.

In this work, it has been determined that for $[\text{Mn}(\text{NH}_3)_6](\text{ClO}_4)_2$, the values of phase transition temperature and lattice parameter a very well fit the graph of vs. a outlined earlier for the family of $[\text{M}(\text{NH}_3)_6](\text{ClO}_4)_2$ compounds.

The investigated sample is unstable in time and temperature. Thermal gravimetry analysis (TG) and DSC measurement informed us that deamination process begins only just at ca. 398 K and above 538 K the decomposition with explosion of manganese(II) perchlorate was observed.

Appearing of the two new bands (splitting of δ_{s} ($\text{HNH})F_{1u}$ mode) in the FT-MIR spectra at the vicinity of $1,200 \text{ cm}^{-1}$, suggests that the phase transition crystal structure undergoes a change.

Acknowledgements The infrared absorption (FT-MIR) researches were carried out with the equipment purchased thanks to the financial support of the European Regional Development Fund in the framework of the Polish Innovation Economy Operational Program (contract no. POIG.02.01.00-12-023/08).

Open Access This article is distributed under the terms of the Creative Commons Attribution License which permits any use, distribution, and reproduction in any medium, provided the original author(s) and the source are credited.

References

1. Migdał-Mikuli A, Mikuli E, Rachwalska M, Hodorowicz S. Investigation of the phase situation in polycrystalline $[\text{Mg}(\text{NH}_3)_6](\text{ClO}_4)_2$ by adiabatic calorimetry and X-ray diffraction methods. *Phys Status Solidi A*. 1978;47:57–64.
2. Hodorowicz S, Ciechanowicz-Rutkowska M, Janik JM, Janik JA. The X-ray powder investigation of phase transitions in $[\text{Ni}(\text{NH}_3)_6](\text{ClO}_4)_2$. *Phys Status Solidi*. 1977;43:53–7.
3. Rachwalska M, Janik JM, Janik JA, Pytasz G, Waluga T. Specific heat of solid $[\text{Ni}(\text{NH}_3)_6](\text{ClO}_4)_2$ in the temperature range from 115 to 300 K. *Phys Status Solidi A*. 1975;30:K81–2.
4. Hetmańczyk J, Migdał-Mikuli A, Hetmańczyk Ł. Phase transition and molecular motions in $[\text{Ca}(\text{NH}_3)_6](\text{ClO}_4)_2$. *Ann Polish Chem Soc*. 2007;358–61. ISBN 978-83-922424-7-5.
5. Hetmańczyk J, Hetmańczyk Ł, Migdał-Mikuli A, Mikuli E, Natkanić I. Phase transition in $[\text{Ca}(\text{NH}_3)_6](\text{ClO}_4)_2$ studied by neutron scattering methods and far infrared spectroscopy. *J Alloy Compd*. 2011;509:6545–50.
6. Migdał-Mikuli A, Mikuli E, Wróbel S, Hetmańczyk Ł. DSC Investigations of the phase transitions of $[\text{M}(\text{NH}_3)_6](\text{ClO}_4)_2$ and $[\text{M}(\text{NH}_3)_6](\text{BF}_4)_2$, where $\text{M} = \text{Co}$ and Cd . *Z. Naturforsch*. 1999;54:590–4.
7. Wyckoff RWG. *Crystal Structures*. 2nd ed., vol. 3. Interscience Publishers, New York; 1965.
8. Janik JM, Janik JA, Migdał-Mikuli A, Mikuli E, Otnes K. Neutron quasielastic scattering results for $[\text{Me}(\text{NH}_3)_6](\text{XY}_4)_2$, $[\text{Me}(\text{NH}_3)_6](\text{XY}_3)_2$ and $[\text{Me}(\text{NH}_3)_6](\text{XY}_2)_2$ compounds, compared with the calorimetric and Raman line width data—a new analysis. *Phys B*. 1991;168:45–52.
9. Dynowska E, Stankowski J. X-ray study on the structural phase transition in nickel hexammine perchlorate. *Phys Status Solidi A*. 1979;52:381–6.
10. Patil KC, Pai Verneker VR, Jain SR. Metal perchlorate amines: thermal and infrared studies. *Thermochim Acta*. 1976;15:257–60.
11. Smith GF, Koch EG. Darstellung und Eigenschaften der Perchloratamine der Erdalkalimetalle. *Z Anorg Chem*. 1935;223:17–27.
12. Mikuli E, Migdał-Mikuli A, Wróbel S. Phase transitions in crystalline $[\text{Me}(\text{H}_2\text{O})_6](\text{BF}_4)_2$. Part I ($\text{Me} = \text{Mn}, \text{Fe}, \text{Co}, \text{Ni}$ and Zn). *Z Naturforsch*. 1999;54:225–8.
13. Shirley R. *The CRYSFIRE system for automatic powder indexing: user's manual*. Guildford, Surrey: The Lattice Press; 2000.
14. Werner PE, Eriksson L, Westdahl M. TREOR, a semi-exhaustive trial-and-error powder indexing program for all symmetries. *J Appl Crystallogr*. 1985;18:367–70.
15. Le Bail A, Duroy H, Fourquet JL. Ab-initio structure determination of LiSbWO_6 by X-ray powder diffraction. *Mater Res Bull*. 1988;23:447–52.
16. Rodriguez-Carvajal J. Recent advances in magnetic structure determination by neutron powder diffraction. *Phys B*. 1993;192:55–69.
17. Stankowski J. Structure phase transitions in $\text{Me}(\text{NH}_3)_6\text{X}_2$. *Mater Sci II*. 1976;11(3):57–62.
18. Migdał-Mikuli A, Hetmańczyk J. Thermal behavior of $[\text{Ca}(\text{H}_2\text{O})_4](\text{ClO}_4)_2$ and $[\text{Ca}(\text{NH}_3)_6](\text{ClO}_4)_2$. *J Thermal Anal Calorim*. 2008;91:529–34.
19. Migdał-Mikuli A, Szostak E, Paweł Bernard P. Thermal analysis, phase transitions and molecular reorientations in $[\text{Sr}(\text{OS}(\text{CH}_3)_2)_6](\text{ClO}_4)_2$. *J Thermal Anal Calorim*. 2014;115:443–9.
20. Mikuli E, Liszka-Skoczylas M, Hetmańczyk J, Szklarzewicz J. Thermal properties, phase transitions, vibrational and reorientational dynamics of $[\text{Mn}(\text{NH}_3)_6](\text{NO}_3)_2$. *J Thermal Anal Calorim*. 2010;102:889–97.
21. Mikuli E, Migdał-Mikuli A, Majda D. Thermal decomposition of polycrystalline $[\text{Ni}(\text{NH}_3)_6](\text{NO}_3)_2$. *J Thermal Anal Calorim*. 2013;112:1191–8.
22. Lovesey SW. Dynamics of solids and liquids by neutron scattering. In: Springer T, editor. *Topics in current physics*, vol. 3. Berlin: Springer-Verlag; 1977.
23. Nakamoto K. *Infrared and Raman spectra of inorganic and coordination compounds*. 5th ed. New York: Wiley-Interscience Publication; 1997.
24. Migdał-Mikuli A, Mikuli E, Barańska M, Hetmańczyk Ł. Vibrational spectrum and molecular structure of $[\text{Cu}(\text{NH}_3)_5](\text{ClO}_4)_2$. *Chem Phys Lett*. 2003;381:329–34.
25. Drużbicki K, Mikuli E. Experimental (FT-IR and FT-RS) and theoretical (DFT) studies of molecular structure and internal modes of $[\text{Mn}(\text{NH}_3)_6](\text{NO}_3)_2$. *Spectrochim Acta A*. 2010;77:402–10.
26. Janik JM, editor. *Fizyka chemiczna*. PWN, Warszawa; 1989 (in polish).
27. Janik JA, Janik JM, Migdał-Mikuli A, Mikuli E, Rachwalska M, Stanek T, Otnes K, Fimland BO, Svare I. Calorimetry, proton magnetic resonance and quasielastic neutron scattering studies of $[\text{Mg}(\text{NH}_3)_6](\text{NO}_3)_2$. *Phys B*. 1983;122:315–20.